Theory of Low-Energy Pion-Pion Scattering. II*

KYUNGSIK KANG
Department of Physics, Brown University, Providence, Rhode Island
(Received 25 February 1965)

We have extended the previously published pion-pion calculations by solving numerically the coupled s- and p-wave equations based on a method of the inverse amplitude, to see if the lower partial waves near threshold converge to definite values. Elastic unitarity is still used for the right-hand cut. Numerical calculations show that the s- and p-wave scattering lengths are very much the same as those obtained before by using only the left-hand singularities chosen to have the correct functional forms near the branch point; however, the position and the width of the p-wave resonance energy are substantially improved. Solutions exhibit results as a function of λ similar to those found previously; a p-wave attraction corresponds to a strong s-wave attraction. Thus we find that the procedure of constructing the amplitude developed in the earlier paper is convincing.

I. INTRODUCTION

IN an attempt to make a limited examination of the pion-pion scattering problem, a procedure was described in a previously published paper,[1] showing how one could write down an amplitude, which satisfied manifestly the analyticity and unitarity requirement in a single channel in the low-energy region, and then make use of crossing symmetry to obtain self-consistency conditions for determination of parameters in the original amplitude. In addition to unitarity, analyticity, and crossing symmetry, there were two other essential features introduced in practical construction of the partial-wave amplitudes. *Firstly*, the partial-wave expansion was terminated at l_m. In particular, the d waves were neglected in carrying out the zeroth- and first-derivative conditions at the symmetry point, while they were included in the second-derivative conditions in the scattering-length approximation. Although the estimated d-wave amplitudes were found to be not very significant at the symmetry point, crossing symmetry was then satisfied only approximately, as is generally the case. *Secondly*, the explicit consideration of higher energy regions in both positive and negative directions was suppressed by using a q_lth-order polynomial and regulating both the right-hand and left-hand integrals. Moreover, the nearby left-hand singularities were chosen so as to preserve the correct functional forms near the branch point. The better we explored the left-hand-cut prescription and inelastic processes, the more realistic a q_l would be obtained. The present paper is devoted to a discussion of the convergence problem of our formulation in Paper I. While still keeping the problem elastic, we have worked out the (nearby) left-hand cut through the crossing relation by machine calculation. In particular, the same l_m and q_l are adopted in numerical calculations of the coupled s- and p-wave amplitudes. It is the purpose of this paper to see how well the lower partial waves near threshold converge to definite values, for then we will find the procedure developed in Paper I convincing.

Upon making a numerical evaluation for the left-hand discontinuities, the number of parameters will be reduced compared to before, and therefore fewer conditions will be needed in determining parameters. The remaining conditions will be used to check self-consistency. The solutions will be characterized by one parameter λ, again as before. The range of this parameter, representing the magnitudes of the s-wave amplitudes at the symmetry point, was discussed in Paper I, and is modified in the present paper by attributing strong s-wave attraction in the $I=0$, $l=0$ state to the existence of a pole on the unphysical sheet.

In Sec. II, the integral equations are described and the additional assumptions that are introduced in the practical case are discussed. Section III considers the approximate crossing conditions and the range of the coupling constant λ. The numerical iteration scheme which will be used to obtain a numerical solution to the coupled s- and p-wave equations is developed in Sec. IV. Section V contains the results of the numerical iteration which are compared with those in Paper I. Finally, in Sec. VI, concluding remarks are given.

II. THE INTEGRAL EQUATIONS FOR THE PARTIAL-WAVE AMPLITUDES

In I, the partial-wave amplitude for orbital angular momentum l and isotopic spin I was given by[2]

$$A_l^I(\nu)=\nu^l[M_l^I(\nu)-i\rho_l^I(\nu)\theta(\nu)]^{-1}, \quad (1)$$

where

$$M_l^I(\nu)=[\nu^{2l+1}/(\nu+1)]^{1/2}\cot\delta_l^I(\nu), \quad (2)$$

and

$$\rho_l^I(\nu)=-R_l^I(\nu)[\nu^{2l+1}/(\nu+1)]^{1/2} \quad \text{for} \quad \nu>0. \quad (3)$$

The function $R_l^I(\nu)$ is the ratio of the total partial-wave cross section to the elastic partial-wave cross section, and is unity in the elastic approximation, which we shall make throughout.

* Work supported by the U. S. Atomic Energy Commission.

[1] K. Kang, Phys. Rev. 134, B1324 (1964), to which the reader is referred for additional references. This paper is referred to as I throughout.

[2] The notation and units are those of I.

The implicit solution of (1) was given by

$$F_l^I(\nu)=\sum_{p=0}^{q_l} a_p\nu^p+\frac{\nu^{N+1}}{\pi}\int_0^R \frac{\rho_l^I(\nu')}{\nu'^{N+1}(\nu'-\nu)}d\nu'$$
$$+\frac{\nu^{M+1}}{\pi}\int_{-L}^{-1}\frac{\rho'_l{}^I(\nu')}{\nu'^{M+1}(\nu'-\nu)}d\nu'+\frac{1}{2\pi i}\int_{\text{circle}}\frac{F_l^I(\nu')}{\nu'-\nu}d\nu', \quad (4)$$

where the function $F_l^I(\nu)$ is defined by

$$F_l^I(\nu)=\nu^l/A_l^I(\nu), \quad (5)$$

and

$$\rho'_l{}^I(\nu)=-\nu^l\,\mathrm{Im}A_l^I(\nu)/|A_l^I(\nu)|^2, \quad \text{for} \quad \nu<-1. \quad (6)$$

The absorptive amplitude in (6) is given by

$$\mathrm{Im}A_l^I(\nu)=\frac{2}{\nu}\int_0^{-\nu-1}d\nu' P_l\left(1+2\frac{\nu'+1}{\nu}\right)$$
$$\times\sum_{I'}\chi_{II'}\sum_{l'}(2l'+1)P_{l'}\left(1+2\frac{\nu+1}{\nu'}\right)\mathrm{Im}A_{l'}^{I'}(\nu'), \quad (7)$$

where $(X_{II'})$ is the well-known 3×3 crossing matrix. The cutoff parameters R and $-L$ in (4) are, in principle, taken at some values where the elastic unitarity and the convergence of (7) begin to fail, respectively. However, by proper introduction of the regularization factors ν^{N+1} and ν^{M+1} on $\rho_l^I(\nu)$ and $\rho'_l{}^I(\nu)$, respectively, and of a polynomial with q_l+1 terms where q_l is the larger of the two integers N and M, it is hoped that sensitive dependence on the cutoff values of the dispersion integrals is eased, so that one may take $R=+\infty$ and $-L=-\infty$ for convenience. Furthermore, the last term in (4), which is the contribution from the large circle of the contour in the complex plane, can always be approximately absorbed into the polynomial in the low-energy approximation.

As in Paper I, it will be assumed that s and p waves are dominant in both direct and indirect channels, and $N=M=l$. Then, in the lth angular-momentum state, there will occur $l+1$ constants in the solution (4).

Under the assumptions we have made, the integral equations become, for the two s waves,

$$F_0^I=\alpha_I+f(\nu)+L_0^I(\nu)$$
$$+i[-\rho_0^I(\nu)\theta(\nu)+\rho'_0{}^I(\nu)\theta(-\nu-1)], \quad (I=0,2), \quad (8)$$

and for the p wave,

$$F_1^1(\nu)=\alpha_1+\beta\nu+\nu f(\nu)+L_1^1(\nu)$$
$$+i[-\rho_1^1(\nu)\theta(\nu)+\rho'_1{}^1(\nu)\theta(-\nu-1)], \quad (9)$$

where

$$f(\nu)=(2/\pi)[\nu/(\nu+1)]^{1/2}\ln[(\nu+1)^{1/2}+(\nu)^{1/2}],$$
$$\text{for} \quad \nu>0 \quad \text{or} \quad \nu<-1$$
$$=(2/\pi)[-\nu/(1+\nu)]^{1/2}\tan^{-1}[(1+\nu)/(-\nu)]^{1/2},$$
$$\text{for} \quad -1<\nu<0, \quad (10)$$

$$L_0^I(\nu)=\frac{\nu}{\pi}P\int_{-\infty}^{-1}\frac{\rho'_0{}^I(\nu')}{\nu'(\nu'-\nu)}d\nu', \quad (11)$$

and

$$L_1^1(\nu)=\frac{\nu^2}{\pi}P\int_{-\infty}^{-1}\frac{\rho'_1{}^1(\nu')}{\nu'^2(\nu'-\nu)}d\nu'. \quad (12)$$

It is observed that our amplitudes (8) and (9) contain four parameters, whereas in Paper I there were three additional parameters due to parametrization of the left-hand singularities. After having obtained solutions for s and p waves, we may ask whether an approximate crossing symmetry is maintained in the course of the numerical calculations. This can be done by taking s- and p-wave solutions to calculate the nearby left-hand singularities from the crossing relations (7) and by comparing them with the defining equations,

$$\mathrm{Im}A_l^I(\nu)=-\mathrm{Im}(A_l^I)^{-1}/|(A_l^I)^{-1}|^2. \quad (13)$$

The two absorptive amplitudes should not be very different from each other in the nearby region where $-\nu$ is smaller than 9. It should be mentioned that in the present paper, these equations will not be used as conditions to determine parameters. Instead they will be used to show the consistency of our solutions.

III. SYMMETRY-POINT CONDITIONS AND THE PION-PION COUPLING CONSTANT

If d and higher waves are small, then one obtains from crossing symmetry[3] that at $\nu=-\frac{2}{3}$

$$A_0{}^0=\tfrac{5}{2}A_0{}^2 \quad (14)$$

and

$$-9A_1{}^1=\frac{\partial A_0{}^0}{\partial\nu}=-2\frac{\partial A_0{}^2}{\partial\nu}. \quad (15)$$

Thus by giving the s-wave amplitude $A_0{}^0$ the value -5λ at the symmetry point, the conditions (14) and (15) provide four independent conditions. The constant λ is sometimes referred to as the pion-pion coupling constant. For a given λ, (14) determines the two s-wave parameters which in turn will be used in determining the two p-wave parameters from the two independent conditions (15).

By taking into account a small effect from d waves in the scattering-length approximation, one gets a single second-derivative condition at the symmetry point;

$$(\partial^2/\partial\nu^2)(A_0{}^0-\tfrac{5}{2}A_0{}^2)=27A_1{}^1+18(\partial A_1{}^1/\partial\nu). \quad (16)$$

We will not attempt to use (16) to determine the parameters, as this will be used to test the consistency of the theory.

The range of λ, $-0.3\leqslant\lambda<0.1$, was found in Paper I to be self-consistent. For this range of λ values, strong s-wave attraction was exhibited for $I=0$, $l=0$, while

[3] G. F. Chew and S. Mandelstam, Nuovo Cimento **19**, 752 (1961).

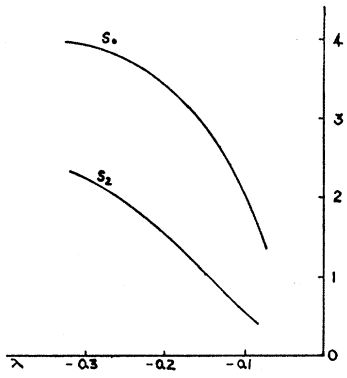

FIG. 1. Position of poles of the s waves on the unphysical sheet as a function of λ. Notice that $\nu_I=\frac{1}{4}s_I-1$.

a p-wave resonance was generated.[4] It is well known that a positive scattering length larger than the force range requires a pole on the unphysical sheet. In this regard, several authors[5] argued that an antibound state would occur in the $I=0$, $l=0$ state, just under the elastic threshold. Although this may not give any new information other than that contained in the original effective-range formula, it is nevertheless interesting to see if this idea limits the range of λ when compared with experiment.

An antibound state in a partial wave $A_l^I(\nu)$ is a pole that appears between $\nu=-1$ and $\nu=0$ on the second Riemann sheet. The analytic continuation of $A_l^I(\nu)$ through the elastic cut into the second Riemann sheet is given by[6]

$$C_l^I(\nu)=A_l^I(\nu)[1-2(-\nu/1+\nu)^{1/2}A_l^I(\nu)]^{-1}, \quad (17)$$

for $-1<\nu<0$. Then the condition for a pole of $C_l^I(\nu)$ at some ν_m is

$$A_l^I(\nu_m)=\tfrac{1}{2}[(\nu_m+1)/(-\nu_m)]^{1/2}, \text{ for } -1<\nu_m<0. \quad (18)$$

The condition (18) was solved for the two s waves of Paper I, and the mass squares s_0 and s_2 of the $I=0$ and $I=2$ antibound states are plotted in Fig. 1. The $I=2$ s-wave state also exhibits an antibound state; however, it is much further from the threshold than the $I=0$ s-wave state. In general, the range $-0.3\leqslant\lambda\leqslant-0.1$ gives an $I=0$ s-wave scattering length which agrees well with the experimental value obtained by Booth and Abashian.[7] No $I=1$ p-wave antibound state was found.

The numerical calculation is carried out for this range of λ. We shall seek solutions with parameters α_1 and β which satisfy the conditions (15) under numerical iteration. Each solution will be checked for consistency by observing if (16) is satisfied. In fact, this can be done by recalculating α_1 and β from the first relation of (15) and (16), when the second relation of (15) is satisfied under iteration, and by comparing them with those satisfying the two conditions of (15). The discrepancy between the two sets of parameters obtained in this way may be attributed to the higher partial waves that are neglected in deriving the symmetry-point conditions. So long as the higher partial waves are small in the nearby region, they should not differ very much from each other, and we shall see that this is indeed so in the present calculation.

IV. THE ITERATION SCHEME

In order to yield rapid convergence, the iteration scheme is started with the solutions obtained in Paper I. In particular, the starting functions for $\rho'_l{}^I(\nu)$ and $L_l^I(\nu)$ are given by (II.12), (II.13), (II.20), and (II.21) of Paper I.

By using new variables

$$y=(1+\nu)^{-1/2}, \quad \text{for} \quad \nu>0, \quad (19)$$

and

$$x=(-\nu)^{-1/2}, \quad \text{for} \quad \nu<-1, \quad (20)$$

the absorptive parts of the s and p waves on the left-hand cut are then found by (7):

$$\mathrm{Im}A_l^I(-x^{-2})=4x^2\int_1^x y^{-3}P_l(1-2x^2y^{-2})$$
$$\times\sum_{I'}x_{II'}\sum_{l'}(2l'+1)P_{l'}\left(1-2\frac{y^2(1-x^2)}{x^2(1-y^2)}\right)$$
$$\times\mathrm{Im}A_{l'}{}^{I'}(y^{-2}-1)dy, \quad (21)$$

which in turn is used to find a new function $\rho'_l{}^I(\nu)$ from (6),

$$\rho'_l{}^I(-x^{-2})=-(-x^{-2})^l\,\mathrm{Im}A_l^I(-x^{-2})/|A_l^I(-x^{-2})|^2. \quad (22)$$

Here, in the first cycle of the iteration, we have used Eqs. (II.20) and (II.21) of Paper I to obtain $\mathrm{Im}A_{l'}{}^{I'}(y^{-2}-1)$, which appears under the integral of (21). To evaluate $\mathrm{Re}A_l^I(-x^{-2})$, the functions (II.12), (II.13), (II.20), and (II.21) of the earlier paper are used to start with. Then from this function $\mathrm{Re}A_l^I(-x^{-2})$ and (21), the function $A_l^I(-x^{-2})$ is readily obtainable and thus $\rho'_l{}^I(-x^{-2})$ of (22) is computed. The procedure that

[4] Positive values of λ give rise to negative values for α_0 and α_2 and do not exhibit the resonance behavior in the p-wave state. Some field-theoretic model calculations claim λ to be positive, for example, M. Alexanian and M. Wellner, Phys. Rev. **137**, B155 (1965).

[5] D. Atkinson, Phys. Letters **6**, 69 (1964); S. Ciulli and GR. Ghika, Phys. Letters **11**, 336 (1964).

[6] R. Oehme, Phys. Rev. **121**, 1840 (1961).

[7] N. E. Booth and A. Abashian, Phys. Rev. **132**, 2314 (1963). They obtained the $I=0$ s-wave scattering length $a_0=2\pm1$ from experiment. H. J. Schnitzer, Phys. Rev. **125**, 1059 (1962), has used a model based on static theory to extract π-π scattering lengths from total cross sections and angular distributions of $\pi+N\to2\pi+N$, and obtained two solutions for the scattering lengths of the $I=0$ s wave, $I=1$ p wave, and $I=2$ s wave: (0.5, 0.7, 0.16) and (0.65, 0.07, −0.14). J. Hamilton, P. Menotti, G. C. Oades, and L. L. J. Vick, Phys. Rev. **128**, 1881 (1962), have pointed out shortcomings in Schnitzer's analysis and in particular that Schnitzer's analysis tends to underestimate the $I=0$ s-wave scattering length.

we have employed in the first cycle will take into account $A_l^I(-x^{-2})$ as a function of x. Also some contribution of the left-hand cut is included in the starting cycle. This feature was completely absent in Paper I. There, in order to obtain Eqs. (II.12) and (II.13), we consistently made a constant approximation for the function $A_l^I(\nu)/\nu^l$ near $|\nu|\approx+1$: By starting with $\mathrm{Im}A_l^{I'}(\nu_t)$ $\sim(\nu_t^{2l+1}/(\nu_t+1))^{1/2}$, the function $\mathrm{Im}A_l^I(\nu_s)$ was obtained near $\nu_s\approx-1$ from Eq. (I.34). Then $\rho'_l{}^I(\nu_s\approx-1)$ was computed from Eq. (II.6) with again a constant approximation for $|A_l^I(\nu_s)|^2$ near $\nu_s\approx-1$. The new functions (22) are used to evaluate the left-hand-cut contributions $L_l^I(\nu)$ of the s and p waves in both the right- and left-hand energy regions; in the physical region

$$L_l^I(y^{-2}-1)=(2/\pi)[(1-y^2)y^{-2}]^{l+1}\int_0^1\{[y^2(-x^2)^{l+1}\rho_l{}'^I(-x^{-2})]/x[y^2(x^2-1)-x^2]\}dx, \quad (23)$$

and in the unphysical region

$$L_l^I(-x^{-2})=(2/\pi)(-x^{-2})^l\times P\int_0^1\{(-z^2)^{l+1}\rho'_l{}^I(-z^{-2})/z[x^2-z^2]\}dz. \quad (24)$$

These functions (23) and (24) will be used to calculate (21) and (22) in the next cycle, with the new s-wave parameters adjusted through the condition (14) for given values of λ. Finally, the s- and p-wave phase shifts become in terms of the calculated L_l^I functions,

$$M_0{}^I(y^{-2}-1)=\alpha_I+f(y^{-2}-1)+L_0{}^I(y^{-2}-1), \quad (I=0,2) \quad (25)$$

and

$$M_1{}^1(y^{-2}-1)=\alpha_1+(y^{-2}-1)[\beta+f(y^{-2}-1)]+L_1{}^1(y^{-2}-1). \quad (26)$$

Starting from the parameters obtained in Paper I for given values of λ, the numerical iteration is performed to determine the functions $\rho'_l{}^I$ and L_l^I. In each iterative cycle, the condition (14) is imposed to readjust the s-wave parameters.[8] Then α_1 and β are varied in a systematic manner until the conditions (15) are satisfied. The final values of the p-wave parameters which are determined in this way are checked for consistency with (16). In particular, they are compared with those obtained from the first relation of (15) and (16).

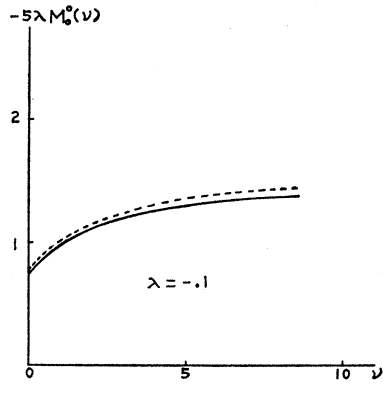

FIG. 2. Comparison of the $I=0$ s-wave phase shift. The dashed curve is the previous solution and the solid curve is from the present calculation.

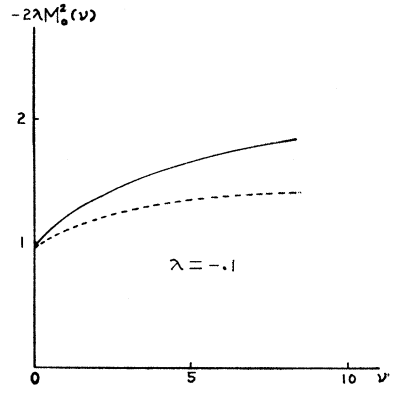

FIG. 3. $I=2$ s-wave phase shift. (See caption of Fig. 2.)

V. RESULTS AND DISCUSSIONS

The integral equations (8) and (9) have been solved numerically on the Brown University IBM-7070 computer. In the range of integration, the variable x is represented by 30 mesh points. The program is started by evaluating functions (22) with L_l^I obtained in Paper I. The convergence is dependent on the values of λ, α_1, and β, and in general, the larger the value of λ, the faster the convergence. For the range of λ, $-0.3\leqslant\lambda\leqslant-0.1$, usually the amplitudes are accurate enough under from three to five iterative cycles. For a given λ, the conditions (15) are imposed for various sets of (α_1,β) and the final sets are those for which conditions (15) are satisfied within 10% accuracy. Each final set of parameters satisfies the condition (16) to an accuracy of 20%. In particular, after the conditions (15) are satisfied, a new set of (α_1,β) is evaluated from the first relation of (15) and (16). Both sets usually agree to within the same accuracy as that to within which condition (16) is itself satisfied. A typical example shows that for $\lambda=-0.1$, the conditions (15) are satisfied by $\alpha_1=175$ and $\beta=-12$, while the consistency check gives $\alpha_1=136.172$ and $\beta=-11.475$. It is generally seen that the larger the value of λ, the less accurately the condition (16) is satisfied. The difference may be due to the higher partial waves neglected in the condition (16). In the earlier calculation, the p-wave parameters for $\lambda=-0.1$ were $\alpha_1=161.0$ and $\beta=-128.9902$. We notice that the value of α_1 obtained in Paper I agrees

[8] Our program is written in a very similar manner to that of B. H. Bransden and J. W. Moffat, Nuovo Cimento 21, 505 (1961). Since we have not made the subtraction at the symmetry point, the condition (14) should be imposed in each cycle of iteration. Their iterative cycle starts with $L_l^I(\nu)$ set equal to zero.

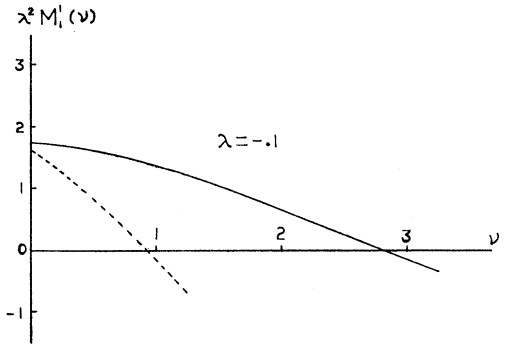

FIG. 4. $I=1$ p-wave phase shift. The position of the p-wave resonance in the present calculation (solid) is significantly improved over that of the previous solution (dashed).

well with the new value; however, the magnitude of β is substantially decreased in the numerical calculation. This tendency is a fact that we have noticed in the earlier paper.

The s-wave scattering lengths are very little changed from those of the earlier calculations. Generally, it is seen that the $I=0$ s-wave phase shift is slightly increased and the $I=2$ s-wave phase shift is decreased. A typical case is shown in Fig. 2 and in Fig. 3, and Table I gives some typical results.

From the integral equations (8) and (9), it is clear that the parameter α is related to the inverse of the scattering length. Our $I=0$ s-wave scattering length is slightly less than 1 (pion Compton wavelength) for $\lambda=-0.1$ and slightly less than 2 for $\lambda=-0.2$. Around $\lambda=-0.2$, we get an $I=0$ s-wave scattering length in good agreement with the experimental value,[7] while around $\lambda=-0.1$, it agrees with the value 1.0 ± 0.3 used by Kacser *et al.*[9] in a study of K_{e4} decays. Our $I=0$ s-wave two-pion state does not show any possibility of having a resonance behavior[10] in the low-energy region; instead, the $I=0$ s-wave phase shift remains approximately constant throughout the ρ-mass region.

TABLE I. s- and p-wave parameters and the positions M_ρ and the widths of the p-wave resonance.

λ	α_0	α_2	α_1	β	M_ρ (MeV)	Γ_ρ (MeV)
−0.1	1.4834	4.8675	175	−12	544	63
−0.2	0.5107	2.2823	28	− 3.5	441	81

[9] C. Kacser, P. Singer, and T. N. Truong, Phys. Rev. **137**, B1605 (1965). These authors obtained agreement with the experimental rate for K_{e4}^+ decay when the $I=0$ s-wave pion-pion interaction is described by a scattering-length approximation with a scattering length $a_0=1.0\pm0.3$.

[10] Some authors assumed a resonance state in the $I=0$ s-wave state to explain the asymmetric $\pi^-\pi^+$ c.m. distribution in ρ^0 production: S. H. Patil, Phys. Rev. Letters **13**, 261 (1964); L. Durand, III, and Y. T. Chiu, Phys. Rev. Letters **14**, 329 (1965). Others found that the asymmetry can be explained by either an s-wave $I=0$ $\pi\pi$ resonance or a large s-wave $I=0$ $\pi\pi$ phase shift near the ρ-meson position: M. Islam and R. Piñon, Phys. Rev. Letters **12**, 310 (1964).

This agrees well with the conclusion of the experimental analysis by Lee,[11] and near $\lambda=-0.2$, the s-wave phase shift coincides with his experimental value.

While the s-wave and p-wave scattering lengths remain almost unchanged, the position of the p-wave resonance is very much improved. For smaller values of $|\lambda|$, corresponding to weaker s-wave attractive forces, the positions of the p-wave resonance are larger. The width Γ_ρ in Table I is given by the formula $\Gamma_\rho=\Gamma[\nu_R^3/(\nu_R+1)]^{1/2}$ where Γ is the reduced width. Again, it is seen that as the value of $|\lambda|$ increases or equivalently as the s-wave forces become more attractive, the p-wave scattering length becomes larger and the p-wave resonance energy becomes smaller. (For $\lambda=-0.3$, the p-wave parameters are $\alpha_1=6$ and $\beta=-34.4$.)

When the value of $|\lambda|$ is small, the s waves are small so that the left-hand cut may be influenced largely by the p wave in indirect channels. Actually, the p-wave absorptive amplitude on the left-hand cut becomes comparable in the nearby region when compared to the s-wave absorptive amplitudes as $|\lambda|$ decreases. Then the situation may resemble the "bootstraps" a little. Since the relations (15), which are obtained from crossing symmetry, determine the p-wave parameters, our procedure then may have some similarities to that of Balázs.[12] In fact, for $\lambda=-0.1$, the p-wave resonance energy turned out to be 544 MeV (as shown in Fig. 4) which is approximately the same as that of Ref. 12.

However, it should be mentioned that the existence of a resonance in our approach arises naturally as a result of direct parameter determination and need not be assumed *a priori*. The situation is different, in this sense, from the bootstrap formalism, where resonances must be assumed from the start. But there seems to be a qualitative possibility in our formalism that the p wave in the crossed channels might produce the most important part of the force needed to produce a resonant p wave in the direct channel, when s waves are of weak attraction.

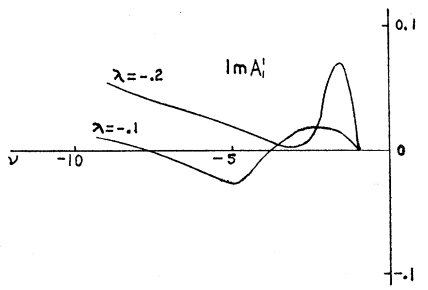

FIG. 5. The p-wave left-hand cut for a weak and a moderately strong coupling. As the values of $|\lambda|$ increase, the sign changes of the left-hand cut disappear.

[11] Y. Y. Lee, University of Michigan Technical Report No. 04938-1-T, 1964 (unpublished).

[12] L. A. P. Balázs, Phys. Rev. **128**, 1939 (1962).

The possible approximate resemblance to the bootstrap situation, when s waves are small, is seen by observing the sign changes of the left-hand cut in the p wave. Figure 5 shows that for smaller $|\lambda|$, $\mathrm{Im}A_1^1$ has two changes of sign. However, as $|\lambda|$ increases, the zeros tend to disappear. The behavior of the p-wave left-hand cut when s waves are small agrees with the conclusions of Jin and Martin[13] in the case of bootstraps.

Table I shows that our width values for the weak and moderately strong s waves are nearer to the value of the width from experiments[11,14] than those from the low-energy bootstrap system.[15] The difference may be due to s waves of moderately strong attraction.

While our amplitudes satisfy elastic unitarity exactly, crossing symmetry is satisfied only approximately. To see this, in Fig. 6 we have plotted $\mathrm{Im}A_l^I$ on the left-hand cut, for a moderately attractive coupling, calculated from the crossing relation (7) and the defining Eq. (13). It is seen that the s waves are well approximated to satisfy crossing symmetry up to the considerable-energy region. However, the two p-wave left-hand cuts slowly become different from each other after $\nu=-5$. We will not attempt any discussion on this since it has already been treated.[16] Instead, we only mention the fair agreement to the crossing relation in the nearby region.

In order to understand that the lower partial waves near the threshold are very similar to those of Paper I where the left-hand cuts are kept to give a correct functional form near the branch point, curves of $\mathrm{Im}(A^I)^{-1}$ are plotted in Fig. 7 and compared with those of the earlier paper for $\lambda=-0.2$. Clearly, in a method based on the inverse amplitude, these curves correspond to the "potential." It is observed that the areas bounded by the two curves are not very different, although the potential in the p-wave state used in I has no resemblance to the numerically calculated potential. Thus the partial-wave amplitudes near the threshold remain more or less unchanged. From this, it may follow

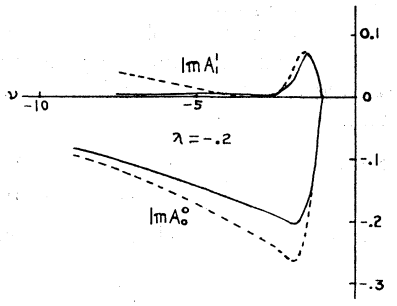

FIG. 6. The left-hand cuts evaluated from crossing symmetry (dashed) and from the defining equation (solid) for a moderately strong coupling.

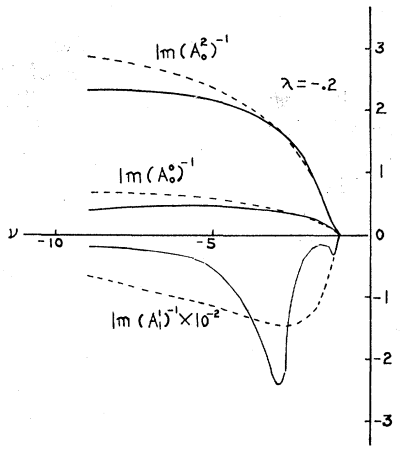

FIG. 7. $\mathrm{Im}[A_l^I(\nu)]^{-1}$ in the present calculation (solid), on the left-hand cut, are compared with those (dashed) used in I.

that approximating the left-hand singularities so that they have a correct functional form near the branch point is not unreasonable as far as an accurate representation of the amplitude for $|\nu|\leqslant 1$ is concerned. However, the prediction of the position and the width of the p-wave resonance is already much improved upon making a better evaluation of the left-hand cut in this elastic approximation.

VI. CONCLUDING REMARKS

In the present calculations, we have still kept only the lowest two partial-wave states. The effect due to the higher partial waves to these amplitudes in the low-energy region is estimated to be about 20%. This was obtained by checking to what extent the final solutions satisfy the second-derivative condition. Thus the second-derivative condition is not used to select out the final parameter λ, since this condition itself is inexact. It is seen that this condition is better satisfied for weak and moderate s-wave attraction. Upon making an improved evaluation of the left-hand cut, the scattering lengths of both the s- and p-wave amplitude are not much changed from those we obtained by using only correct functional forms near the branch point for the left-hand cut; however, the position and width of the p-wave resonance are much improved for weak and moderately strong s-wave attraction. For stronger s-wave attraction, the s-wave and p-wave scattering lengths become larger and the position of the p-wave resonance energy moves toward zero energy.

We have thus seen that for $|\nu|<1$, the "potential" chosen to have a correct functional form near the branch point gives a sufficiently accurate amplitude, and that a better expression for the potential improves the accuracy. This, we feel, justifies our procedure of constructing the scattering amplitude. That is, because of the uncertainty of the singularities in the high-energy region, we choose to incorporate this uncertainty in the

[13] Y. S. Jin and A. Martin, Phys. Rev. **135**, B1369 (1964).
[14] B. C. Maglić, L. W. Alvarez, A. H. Rosenfeld, and M. L. Stevenson, Phys. Rev. Letters **7**, 178 (1961).
[15] For example, M. Bander and G. L. Shaw, Phys. Rev. **135**, B267 (1964).
[16] B. H. Bransden and J. W. Moffat, Phys. Rev. Letters **8**, 145 (1962).

polynomial by suppressing explicit consideration of the higher energy region through regularized integrals, which are cut off at some finite values of the energy up to which the singularities are known. The order of regularization is chosen so that the cutoff dependence of the integrals becomes insensitive, as discussed in Sec. II. The fact that the potentials calculated have no worse behavior in the high-energy region than those used in Paper I, as is seen in Fig. 7, allows us to use the same order of regularization as before. If we knew a representation of inelastic effects, this would have been used to adjust the order of regularization.

That the second-derivative condition is satisfied only approximately by our solution implies the necessity of bringing the d waves into the formulation. Then the symmetry-point conditions will have to be modified. The elastic approximation becomes very poor, since it gives only tiny effects of higher partial waves in the symmetry-point region. Eventually, the inelastic effects should be brought in when higher partial waves are included.

ACKNOWLEDGMENTS

The author is happy to thank Professor David Feldman and Professor Marc Ross for their encouragement and interest in this work, and Professor J. W. Moffat for giving information on the computing program. He is also indebted to Dr. M. M. Islam for discussions and to the staff of the Brown University Computing Laboratory for their cooperation.

PHYSICAL REVIEW VOLUME 139, NUMBER 1B 12 JULY 1965

$SU(3)$ Symmetry, $K \to 2\pi$ Decay Modes, and CP Violation

S. N. Biswas, S. K. Bose, and V. S. Mathur
Center for Advanced Studies in Theoretical Physics and Astrophysics, University of Delhi, Delhi, India
(Received 4 January 1965; revised manuscript received 15 March 1965)

A model for the 2π decay modes of the K meson, based on the assumption of the icosuplet transformation property of the weak Hamiltonian under SU_3, is constructed. The model incorporates CP violation in a natural way.

In this note we propose to construct a model for the nonleptonic two-body decay modes of the K meson based on the $SU(3)$ symmetry. The recent observation[1] of the $\pi^+\pi^-$ decay mode of K_2^0 has established[2] the violation of CP in this decay. Within the framework of $SU(3)$, a possible way of introducing CP violation in weak interactions is to ascribe an icosuplet transformation property[3] to the weak Hamiltonian. With the choice of such a Hamiltonian, one can hope that the K^+ decay into $\pi^+\pi^0$, which goes by a $T=3/2$ spurion, may not require a special treatment over the 2π decay modes of K_1^0. The purpose of this note is to construct such a model and to show that all known 2π decay modes of the K meson can be understood consistently on the basis of this model. We use CPT invariance and work throughout in the limit of exact $SU(3)$.

Our model for the weak Hamiltonian responsible for the decay modes is

$$H=H_1+\epsilon H_2, \tag{1}$$

and the $SU(3)$ transformation properties of H_1, H_2 are

$$H_1\sim 10+10^*, \tag{2}$$

$$H_2\sim i(10-10^*)\,. \tag{3}$$

It is clear that H_1 and H_2 are, respectively, even and odd under CP. Thus H can lead to CP-violating transitions. ϵ is a real parameter which measures the strength of CP violation. Specifically, the relevant spurions responsible for the decay $K\to 2\pi$ transform like the $Y=-1$, $I=\frac{1}{2}$ state in 10, and the $Y=-1$, $I=\frac{3}{2}$ state in 10^*. On the basis of (1)–(3), one can construct the decay matrix elements, using the appropriate spurions. Making use of CPT invariance these matrix elements can be written as

$$\begin{aligned}
&\langle K^+|H|\pi^+\pi^0\rangle=-3/4\sqrt{2}\,\sec\alpha\; a_{27}e^{i(\delta_2-\alpha)}\,,\\
&\langle K^-|H|\pi^-\pi^0\rangle=-3/4\sqrt{2}\,\sec\alpha\; a_{27}e^{i(\delta_2+\alpha)}\,,\\
&\langle K^0|H|\pi^0\pi^0\rangle=\sec\alpha\,\{[(1/20)a_{27}+\tfrac{1}{5}a_8]\\
&\qquad\times e^{i(\delta_0+\alpha)}-\tfrac{1}{2}a_{27}e^{i(\delta_2-\alpha)}\}\,,\\
&\langle \bar K^0|H|\pi^0\pi^0\rangle=\sec\alpha\,\{[(1/20)a_{27}+\tfrac{1}{5}a_8]\\
&\qquad\times e^{i(\delta_0-\alpha)}-\tfrac{1}{2}a_{27}e^{i(\delta_2+\alpha)}\}\,,\\
&\langle K^0|H|\pi^+\pi^-\rangle=\sqrt{2}\,\sec\alpha\,\{-[(1/20)a_{27}+\tfrac{1}{5}a_8]\\
&\qquad\times e^{i(\delta_0+\alpha)}-\tfrac{1}{4}a_{27}e^{i(\delta_2-\alpha)}\}\,,\\
&\langle \bar K^0|H|\pi^+\pi^-\rangle=\sqrt{2}\,\sec\alpha\,\{-[(1/20)]a_{27}+\tfrac{1}{5}a_8]\\
&\qquad\times e^{i(\delta_0-\alpha)}-\tfrac{1}{4}a_{27}e^{i(\delta_2+\alpha)}\}\,.
\end{aligned} \tag{4}$$

[1] J. H. Christenson, J. W. Cronin, V. L. Fitch, and R. Turlay, Phys. Rev. Letters **13**, 138 (1964).

[2] There have been several attempts [J. Bernstein, N. Cabibbo, and T. D. Lee, Phys. Letters **12**, 146 (1964); M. Levy and M. Nauenberg, Phys. Letters **12**, 155 (1964); J. S. Bell and J. K. Perring, Phys. Rev. Letters **13**, 348 (1964)] to understand this experiment in a CP-invariant way.

[3] The terminology is due to B. W. Lee, S. Okubo, and J. Schecter, Phys. Rev. **135**, B219 (1964).